Electronic Supplementary Material (ESI) for Nanoscale.

Maximization of thermal conductance at interfaces via exponentially mass-graded interlayers

Rouzbeh Rastgarkafshgarkolaei[a],[1,*] Jingjie Zhang[b],[2,*] Carlos A. Polanco,[3] Nam Q. Le,[4] Avik W. Ghosh,[2,5] and Pamela M. Norris[c1]

[1] *Department of Mechanical and Aerospace Engineering, University of Virginia, Charlottesville, Virginia 22904, USA*
[2] *Department of Electrical and Computer Engineering, University of Virginia, Charlottesville, Virginia 22904, USA.*
[3] *Materials Science and Technology Division, Oak Ridge National Laboratory, Oak Ridge, Tennessee 37831, USA.*
[4] *National Research Council Research Associateship Programs, Code 6189, U.S. Naval Research Laboratory, Washington, District of Columbia 20375, USA.*
[5] *Department of Physics, University of Virginia, Charlottesville, Virginia 22904, USA.*

(Dated: February 25, 2019)

[a] rr3ay@virginia.edu
[b] jz9wp@virginia.edu
[c] pamela@virginia.edu
[*] These two authors contributed equally

APPENDIX A: SIMULATION DETAILS

The mass-graded interfaces (Fig. 1) are built with a face centered cubic (FCC) crystal structure, with one atom per primitive unit cell and keeping the lattice constant a as well as interatomic force constants invariant. Different materials only differ on their values of atomic mass and those masses (m_j) are varied between the contact atomic masses m_l and m_r according to Eq. 1. All material boundaries are set as perfectly abrupt interfaces. Interatomic interactions are defined using the Lennard-Jones (LJ) potential $U_{LJ}(r_{ij}) = 4\epsilon[(\sigma/r_{ij})^{12} - (\sigma/r_{ij})^{6}]$, with energy scale $\epsilon = 0.0503$ eV, length scale $\sigma = 3.37$ Å, cutoff distance 2.5σ (which includes up to 5^{th} nearest neighbors) and r_{ij} the distance between atoms i and j. Those values are equal to the ones used in our previous work [1]. For harmonic NEGF calculations, interatomic force constants were defined according to 2^{nd} order derivatives of the LJ potential. At $\mathbf{T} = 0$ K, the equilibrium lattice constant is $a = 5.22$ Å. The mass of the left and right contacts are fixed to $m_l = 40$ amu and $m_r = 120$ amu respectively for Figs. 2-8. For Fig. 9 $m_r = 400$.

NEMD simulations are done using LAMMPS MD simulator with 2 fs time-step, on a simulation domain containing $10 \times 10 \times 302$ conventional unit cells. Periodic boundary conditions are imposed along the transverse directions (x and y) and the atomic layers at the edges of the simulation domain in the transport direction (z) are set as walls. Heat is added to the system on the first 50 unit cell layers in z and removed on the last 50 unit cell layers in z using the Langevin thermostat with baths' temperatures $\mathbf{T}_{bath} = (1 \pm 0.1)\mathbf{T}$ and a time constant of 1.07 ps. This prevents potential size effects by ensuring sufficient phonon-phonon scattering. For the simulations at $\mathbf{T} = 2$ K, corresponding to a non-dimensional temperature $k_B\mathbf{T}/\epsilon = 0.003$ (less than 1% the melting temperature), significant size effects can arise due to the lack of phonon thermalization since atomic displacements are small and almost harmonic. To guarantee enough thermalization in our systems, we increase the size of each thermal bath and choose 300 unit cells as the simulation domain thickness. Table S1 shows how thermal conductance changes with the thickness of the simulation domain. At 300 u.c., the change in G is less than the standard deviation of our NEMD simulation results, thus we conclude that using 300 u.c. thickness as our simulation domain guarantees that our results are independent from size effects. We also tested for potential size effects due to the cross section, the thickness of the domain and the thermostat time constant in our previous work [1] and no significant change in the interfacial thermal conductance was noticed.

TABLE S1. Size effects on the thermal conductance of a mass-graded interface determined by our NEMD simulations. Results are for the system with $m_l = 40$ amu, $m_r = 120$ amu and the mass-graded layer with 10 layers N_l and each layer thickness t is equal to 2 unit cells. The conductance values are given in $\mathrm{MWm^{-2}K^{-1}}$. The standard deviation of five independent calculations is the reported error.

	G ($\mathrm{MWm^{-2}K^{-1}}$)				
Thickness (u.c.)	60	90	120	240	300
$\mathbf{T} = 2$ K	88.17 ± 0.47	88.86 ± 1.59	89.04 ± 0.59	91.06 ± 0.93	91.26 ± 0.65
$\mathbf{T} = 30$ K	146.47 ± 1.02	150.66 ± 1.09	155.01 ± 2.51	165.77 ± 5.45	163.95 ± 5.04

Thermal expansion of the system was considered to prevent the influence of thermal driven pressure changes on our thermal transport calculations. To that end, we fit the change in lattice constant with temperature for a set of equilibration runs under zero pressure using isothermal-isobaric ensemble (NPT) [1]

$$a(\mathbf{T}) = 5.2222 + 0.0004\mathbf{T} + 10^{-6}\mathbf{T}^2 - 4 \times 10^{-9}\mathbf{T}^3 \text{Å}. \quad (1)$$

Interfacial thermal conductance is estimated from individual temperature profiles and reported values are averages over five independent NEMD runs, each with a randomly generated initial velocity condition. G equals the heat

flux crossing the junction over the temperature drop, which results from a linear fit of the temperature at each lead extrapolated to the interface.

In the NEGF simulations, we use 100 grid points to sample the 0–20 Trad/s frequency range and 100×100 grid points to sample a FCC conventional unit cell Brillouin zone. This dense frequency and wavevector samplings guarantees the convergence of G. In all NEGF calculations, we excluded the effect from the contact resistance, and the conductances are four-probe measured conductances [1]. This set-up helps us compare the NEGF and NEMD results. Before we started the systematic calculations of the exponential graded systems, we compared our NEGF and MD simulations. For an $m_l = 40$ amu and $m_r = 120$ amu abrupt interface system, we got G =70.14 MW m^{-2} K^{-1} at T =0 K from NEGF calculations and G =71.71±0.36 MW m^{-2} K^{-1} at T =2 K from NEMD. These values are reasonably close considering the temperature difference.

APPENDIX B: ADDITIONAL THEORETICAL ARGUMENTS

An informal proof that an exponential mass-graded junction minimizes the resistance due to all material boundaries can be done in the following way. Assume that the resistance at any individual material boundary is given by a function f that only depends on the mass ratio of the materials at either side of the boundary. Also assume the total resistance R_T due to all the material boundaries is given by the sum of resistances at individual material boundaries:

$$R_T = \sum_i f\left(\frac{m_i}{m_{i+1}}\right). \tag{2}$$

To minimize R_T, we first find the critical points of R_T by equating its first derivatives to 0:

$$\frac{\partial R_T}{\partial m_i} = \frac{1}{m_{i+1}} f' - \frac{m_{i-1}}{{m_i}^2} f' = 0. \tag{3}$$

Since the derivative of f, f', is not necessarily 0, the equation is solved when

$$\frac{1}{m_{i+1}} = \frac{m_{i-1}}{{m_i}^2}, \tag{4}$$

which is equivalent to the geometric mean condition referred in the manuscript:

$$m_i = \sqrt{m_{i-1} m_{i+1}}. \tag{5}$$

Solving the system of equations above (one equation per i), the mass of material i, m_i is given by:

$$m_i = m_l^{(N_l+1-i)/(N_l+1)} m_r^{i/(N_l+1)}, \tag{6}$$

which is equivalent to Eq. 1 in the main manuscript. Proving that the critical point of R_T defined by the equation above is a minimum, requires detailed knowledge of the function f, and goes beyond the scope of the current manuscript. Nevertheless, we expect this critical point to be a minimum based on our previous results, where this is true for the particular case N_l=1 [1] as well as for 1D atomic chains [2]. Another supporting evidence comes from the conductance of the exponential mass-graded junction being larger than that of the linear mass-graded junction. Note that the informal proof outlined above does not directly apply to the systems presented here, since the boundary resistance does not only depend on the mass ratio of the materials at either side of the boundary but also on their minimum cut-off frequency, which is a function of mass (See Eq. 10 on [1]). Nevertheless, on [1] we showed that the boundary resistance depends dominantly on the mass ratio, so the actual minimum resistance is achieved at a condition close to that given by Eq. 1.

APPENDIX C: FIGURES SUPPORTING THE MANUSCRIPT

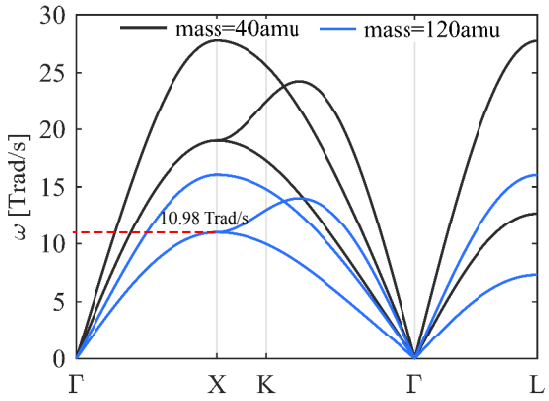

FIG. S1. Phonon dispersions for the materials at either side of the interface. The cutoff frequency for the lightest material on the left is 27.81 Trad/s while for the heaviest material on the right is 16.06 Trad/s. The frequency range, where phonons cross the junction conserving their polarization, is limited by the frequency range of the TA/LA branches of the heavy material. As a result, phonon transmission conserving TA and LA polarization can happen below 10.98 Trad/s and 16.06 Trad/s respectively.

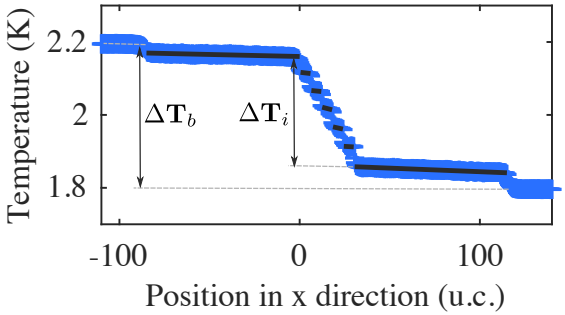

FIG. S2. Temperature profile for an exponential mass-graded system with $t = 6$ u.c. and $N_l = 5$ at $\mathbf{T}$=2 K. The temperature difference between the thermal baths is $\Delta\mathbf{T}_b$= 0.40 K. The temperature across the junction or interface $\Delta\mathbf{T}_i$ is 0.30 K. The total temperature drop at all the boundaries is 93% of $\Delta\mathbf{T}_i$.

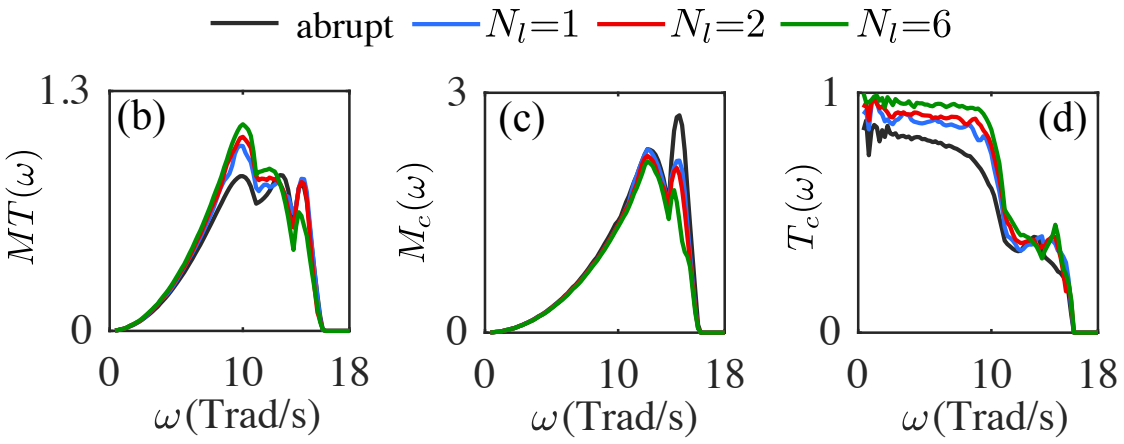

FIG. S3. Enlarged versions of Fig.3(b)-(d) in the paper. NEGF results of (b) number of modes times transmission MT(ω), (c) number of available modes $M_c(\omega)$ and (d) average transmission $T_c(\omega) = \frac{MT(\omega)}{M_c(\omega)}$ when N_l is 0 (abrupt), 1, 2 and 6. All simulations are performed for $t = 6$ u.c.

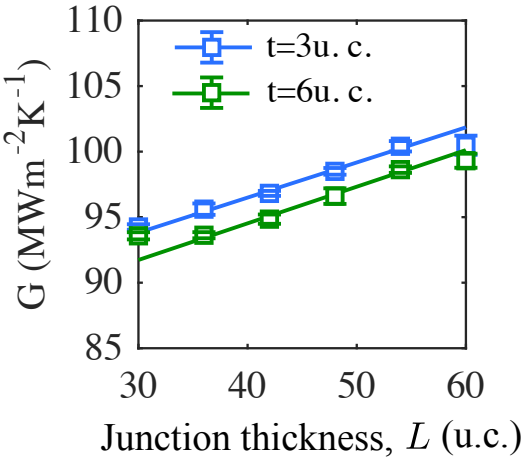

FIG. S4. Interfacial thermal conductance values from NEMD simulations at T = 2 K versus junction thickness. The square markers represent datas from NEMD simulations while the solid lines represent linear fittings to the data.

APPENDIX D: ALL THE NEGF AND NEMD CONDUCTANCE DATA

REFERENCES

[1] C. A. Polanco, R. Rastgarkafshgarkolaei, J. Zhang, N. Q. Le, P. M. Norris, and A. W. Ghosh, "Design rules for interfacial thermal conductance: Building better bridges," Phys. Rev. B, vol. 95, no. 19, p. 195303, 2017.

[2] C. A. Polanco and A. W. Ghosh, "Enhancing phonon flow through one-dimensional interfaces by impedance matching," J. Appl. Phys., vol. 116, no. 8, p. 083503, 2014.

TABLE S2. Harmonic conductance from NEGF simulations G_{hl} (MWm^{-2}K^{-1})

	layer thickness t (u.c.)					
	1	2	3	4	5	6
Number of layers N_l	G_{hl}	G_{hl}	G_{hl}	G_{hl}	G_{hl}	G_{hl}
1	84.13	78.09	76.96	77.04	76.57	76.59
2	85.43	81.67	79.68	79.00	78.42	78.39
3	86.01	81.43	79.28	78.86	78.78	78.63
4	85.33	80.79	79.27	79.09	78.81	78.74
5	84.33	80.47	79.50	79.20	78.76	78.88
6	83.84	80.44	79.80	79.14	78.88	78.84
7	83.46	80.36	80.03	79.18	78.99	78.61
8	83.16	80.36	80.07	79.22	79.05	78.63
9	83.03	80.34	80.04	79.20	79.02	78.67
10	82.95	80.32	79.93	79.26	78.94	78.62
11	82.84	80.30	79.92	79.23	78.87	78.73
12	82.71	80.30	79.77	79.37	78.83	78.65
13	82.56	80.25	79.74	79.28	78.77	78.62
14	82.53	80.32	79.73	79.30	78.80	78.60
15	82.43	80.34	79.66	79.33	78.79	78.58
16	82.35	80.33	79.63	79.28	78.84	78.54
17	82.29	80.33	79.57	79.25	78.84	78.47
18	82.24	80.35	79.54	79.22	78.80	78.51
19	82.20	80.34	79.47	79.14	78.77	78.39
20	82.17	80.39	79.42	79.04	78.77	78.39

TABLE S3. Conductance G from NEMD simulations at **T**=2 K (MWm^{-2}K^{-1}). The conductance of the abrupt interface is 71.71±0.36 MW m^{-2} K^{-1}

	layer thickness t (u.c.)											
	1		2		3		4		5		6	
Number of layers N_l	G	std	G	std	G	std	G	std	G	std	G	std
1	87.38	0.78	81.96	0.83	80.09	1.6	80.59	1.02	82.61	1.2	81.52	0.94
2	89.78	0.43	87	1.03	85.04	0.87	85.95	1.13	86.29	1.19	86.95	0.51
4	91.13	1.37	87.68	1.45	86.82	0.79	88.78	1.4	89.79	0.5	91.5	1.38
5	90.47	0.99	87.01	0.74	89.41	0.85	89.36	1.56	91.2	1.15	93.58	0.62
6	89.33	1.13	88.21	1.27	90.15	0.83	89.82	0.55	92.61	1.28	93.62	0.52
7	89.56	0.88	89.53	1.61	90.19	1.58	91.98	0.63	93.53	1.24	94.85	0.79
8	89.82	1.54	89.31	0.61	92.2	1.4	93.86	0.61	95.29	1.07	96.61	1.33
9	89.49	1.41	90.06	0.7	93.55	1.41	95.22	0.78	96.3	1.87	98.63	0.56
10	89.75	1.29	91.26	0.65	94.25	0.47	97.17	0.32	98.12	1.19	99.3	1.2
12	90.71	0.75	93.14	0.73	95.61	0.97	96.57	1.07	100.95	1.56	N/A	N/A
14	90.82	0.68	94.61	0.47	96.81	0.42	N/A	N/A	N/A	N/A	N/A	N/A
16	91.01	1.48	94.54	0.4	98.49	0.57	101.2	1.5	103.95	1.27	106.62	0.46
18	91.27	1	96.66	1.07	100.41	0.89	N/A	N/A	N/A	N/A	N/A	N/A
20	91.38	0.94	97.31	0.84	100.48	1.64	N/A	N/A	N/A	N/A	N/A	N/A
30	94.37	1.16	101.9	1.25	N/A	N/A	N/A	N/A	N/A	N/A	N/A	N/A
60	101.53	1.76	N/A	N/A	N/A	N/A	N/A	N/A	N/A	N/A	N/A	N/A

TABLE S4. Conductances G from NEMD simulations at **T**=30 K ($MWm^{-2}K^{-1}$).The conductance of the abrupt interface is 102.40±1.70 $MWm^{-2}K^{-1}$.

	layer thickness t (u.c.)											
	1		2		3		4		5		6	
Number of layers N_l	G	std	G	std	G	std	G	std	G	std	G	std
1	134.45	1.27	135.03	1.08	130.48	1.51	133.73	1.89	134.52	0.81	135.25	1.98
2	146.48	1.09	143.99	0.75	144.05	1.47	150.8	2.27	143.7	1.94	148.99	2.02
4	153.32	1.7	156.36	1.62	154.01	2.3	156.11	1.39	156.88	2.75	157.18	0.89
5	157.65	2.62	156.58	1.16	156.78	1.91	163.11	1.78	154.44	0.75	152.23	1.39
6	156.4	1.26	161.84	0.82	160.72	1.54	158	3.44	155.02	0.72	155.63	1.65
7	156.05	2.15	162.87	1.92	166.29	2.15	161.79	0.36	156.98	2.17	156.63	1.23
8	158.07	2.32	165.05	1.27	165.4	1.04	159.27	1.32	154.28	1.62	150.57	0.81
9	161.4	2.77	164.4	1.9	169.3	1.58	160.41	1.26	154.25	2.21	147.21	0.49
10	164.13	2.03	163.95	2.52	164.56	1.27	159.62	0.78	152.1	0.93	144.24	0.76
12	161.89	3.77	164.82	4.76	162.76	3.28	153.5	3.07	144.46	2.42	N/A	N/A
14	164.58	1.46	167.48	3.1	159.43	1.88	N/A	N/A	N/A	N/A	N/A	N/A
16	167.33	6.48	163.47	3.78	157.64	2.51	147.46	4.21	137.37	5.19	122.69	4.26
18	166	6.27	167.26	2.49	154.02	3.78	N/A	N/A	N/A	N/A	N/A	N/A
20	170.24	5.14	162.49	3.97	150.1	0.7	N/A	N/A	N/A	N/A	N/A	N/A
30	167.91	3.01	152.09	3.36	N/A	N/A	N/A	N/A	N/A	N/A	N/A	N/A
60	150.92	2.43	N/A	N/A	N/A	N/A	N/A	N/A	N/A	N/A	N/A	N/A